Catal Lett (2007) 118:254–259
DOI 10.1007/s10562-007-9179-5

A Novel Method for Preparing V-doped Titanium Dioxide Thin Film Photocatalysts with High Photocatalytic Activity Under Visible Light Irradiation

De-En Gu · Bang-Chao Yang · Yong-Da Hu

Received: 17 April 2007 / Accepted: 18 June 2007 / Published online: 17 July 2007

Abstract The liquid phase deposition (LPD) method was successfully used for preparing V-doped TiO_2 thin film photocatalysts. In this simple and easily-controlled process, V-doped anatase TiO_2 thin films were directly deposited on a soda lime glass substrate placed in an aqueous solution containing Ti- and V-fluoro complex ions, followed by annealing. The thin films were analyzed by XRD, XPS, UV-vis. V^{4+} ions were introduced into the lattice of TiO_2 through in-situ substituting Ti^{4+}. The absorption edge of V-doped TiO_2 films shifted to visible light region. The highly efficient photocatalytic activity was verified by the decomposition of methylene blue under visible light irradiation.

Keywords Titanium dioxide thin films · Liquid phase deposition · Vanadium · Visible light photocatalytic activity · Methylene blue

1 Introduction

A titanium dioxide (TiO_2) photocatalyst has gained more and more importance in the past decades due to its excellent capability of degrading a large variety of environmental contaminants such as organics, bacteria, viruses [1, 2], especially following the discovery of the photoinduced water-splitting on TiO_2 [3]. However, the widespread application of TiO_2 as a photocatalyst has been cumbered with its wide band gap (3.2 eV for anatase TiO_2). This requires ultraviolet (UV) irradiation for photocatalytic activity. UV light accounts for a small fraction (~5%) of the sun rays on the surface of the earth comparing with visible light. So, shifting the absorption edge of a TiO_2 photocatalyst from UV to the visible spectral range can provide the groundwork to the development of TiO_2 catalysts with visible light (vis-) photocatalytic activity. Several attempts have been made to develop vis-photocatalytic TiO_2 catalysts [1, 4–7]. Doping of TiO_2 with transition metal ions is one of the important approaches [7–9]. Of the transition metals for doping (V, Cr, Mo, Fe, etc.), V has been one of the frequent topics of investigation because of conspicuous absorption in the visible region [10–14]. The methods for preparing V-doped TiO_2 catalysts are: a sol–gel method, a metal ion-implantation method, a coprecipitation method, and other methods [10–16]. Among these methods, a coprecipitation method and a sol–gel method are widely employed due to being low-cost and easy to execute. A coprecipitation method is often used for preparing V-doped TiO_2 powders [15, 16]. A sol–gel method is frequently used for depositing the V-doped TiO_2 films [11–13]. However, easily-hydrolyzed organic materials, such as titanium isopropoxide [11, 12], are used as starting materials in sol–gel techniques. This makes the sol-gel process hard-controlled.

Since the liquid phase deposition (LPD) method was reported by Kawahara et al. as a novel wet method for preparing a variety of metals oxides [17], it has been used to deposit silica films [18] and non-silica films such as titania [19], and vanadia [20]. In this process, metal oxide thin films or hydroxide thin films are directly deposited on a substrate that is placed in an aqueous solution containing corresponding metal-fluoro complex ions. The films are formed through the hydrolysis reaction of metal-fluoro complex ions. The hydrolysis equilibrium will be shifted

---

D.-E. Gu (✉) · B.-C. Yang · Y.-D. Hu
School of Microeletronics and Solid-state Electronics,
University of Electronic Science and Technology of China,
Chengdu 610054, China
e-mail: gudeen@163.com

towards the metal oxide if the concentration of the hydrogen fluoride is decreased by addition of the fluorine scavengers, such as boric acid or aluminum [17–20]. The LPD method is a very simple and easy-controlled process for fabricating thin films and does not require special equipments, such as sputtering equipments. Since the formation of oxide films occurs in aqueous solutions of metal-fluoro complex, which are the typical homogeneous mixing system, homogeneous composite thin films can be readily prepared by the LPD methods. S. Deki et al. have deposited rare earth-doped Titanium dioxide thin films on glass and Si wafer substrates through the LPD process [21].

In the present study, V-doped anatase TiO_2 thin films, which are highly vis-photocatalytically active, have been successfully deposited on a soda lime glass substrate through the LPD method. The crystallographic structures of the films were characterized by means of X-ray diffraction (XRD). X-ray photoelectron spectroscopy (XPS) was utilized to analyze the chemical status of Vanadium in the V-doped TiO_2 thin films. The optical properties were investigated by UV-vis spectrophotometry. The high vis-photocatalytic activity was detected by the degradation of methylene blue.

2 Experimental

V-doped TiO_2 thin films were fabricated using the LPD method. Ammonium hexafluorotitanate ($(NH_4)_2TiF_6$) and boric acid (H_3BO_3) were separately dissolved in deionized water. Vanadium (*V*) oxide was supersaturated in 5% aqueous solution of hydrofluoric acid. The solution containing 0.2M vanadium ions was obtained. Before the mixing, three kind of the solutions were kept separately at room temperature for 10h. The treatment solutions containing 0.1 $M(NH_4)_2TiF_6$, 0.2 MH_3BO_3, and various concentration vanadium ions are prepared by adding the appropriate amount of ammonium hexafluorotitanate solution and the vanadium ions solution into the boric acid solution. For the samples VT001, VT0025, VT005 and VT01, the molar ratios ($R_{V/Ti}$) of V and Ti ions in treatment solutions are respectively 0.01, 0.025, 0.05, and 0.1. After mixing, the mixed solution was putted into a teflon beaker as the treatment solution. Soda lime glass was used as the substrate. After ultrasonically degreasing and washing, the substrates were vertically placed in the treatment solution, and kept at 30 °C for 20 h. Then they were taken out, washed with deionized water, and dried at 110 °C for 48 h. After annealing at 400 °C in air for 60 min, V-doped TiO_2 films were obtained. For comparison, the undoped TiO_2 thin films were prepared by the similar process just without the addition of V ions.

The XRD patterns of the films were recorded on a Philips X'pert X-ray diffractometer equipped with a thin film attachment, operated at 40 kV (Cu-K_α radiation). XPS measurements were performed on VG MICROLAB MKα. Magnesium K_α radiation was used as the excitation source($h\nu$ = 1253.6eV). For each sample, C1s, O1s, Ti2p, V2p peaks were recorded. All the binding energies were calibrated by the C1s peak at 285.0 eV of the adventitious surface carbon. The optical properties were measured at room temperature by means of an UV-vis spectrophotometer (SHIMADZU, UV2100). UV-vis absorption spectra of V-doped TiO_2 films were recorded in the range of λ = 300nm–800nm.

The photo degradation of methylene blue (MB), as one of the model materials for photocatalytic activity [6, 12, 22], is used to evaluate the photocatalytic activities of the films. A 0.005 mmol/L MB solution was formed by dissolved 3.7 mg MB in 2L de-ionized water. An 100 W incandescent lamp (Philips)without focusing was used as a light source. The light source was placed above the V-doped TiO_2 films in order that the films were irradiated in the normal direction. The distance between the V-doped TiO_2 films and the light source is about 20 cm. The soda lime glass with V-doped TiO_2 thin films was placed into 100 mL 0.005 mmol/L MB solution. Before irradiation, the samples were placed in 0.005 mmol/L MB solution for 30 min at dark, in order to reach absorption equilibrium. During the photo degradation, the solution was stirred by a magnetic stirring apparatus. The decolorization of the solution was determined by an UV-vis spectrometer using wavelength 661.0 nm.

3 Results and Discussion

XRD measurements were performed for all the samples before and after annealing at 400 °C in air for 60 min. No obvious peak was found in the XRD pattern of the as-prepared V-doped TiO_2 thin films (not shown). After annealing at 400 °C for 60 min, the anatase TiO_2 phase can be observed in the XRD patterns of all the samples as shown in Fig. 1. The hump about at the range of 15–35°, present in all the patterns, is due to soda lime glass as the substrate. The intensity of the (101) peak of anatase increased with the V amount. This shows that an introduction of V promotes the growth of anatase TiO_2. It has reported that a small amount of V decreases the crystallization temperature of the anatase TiO_2 [22]. No characteristic peak of vanadium oxides (V_2O_5 and VO_2) were showed in the XRD patterns of the samples obtained from the solutions with $R_{V/Ti}$ less than 0.1, which implies V is incorporated in the lattice of anatase TiO_2 or vanadium oxide is very small and highly dispersed [22]. For the sample VT01,

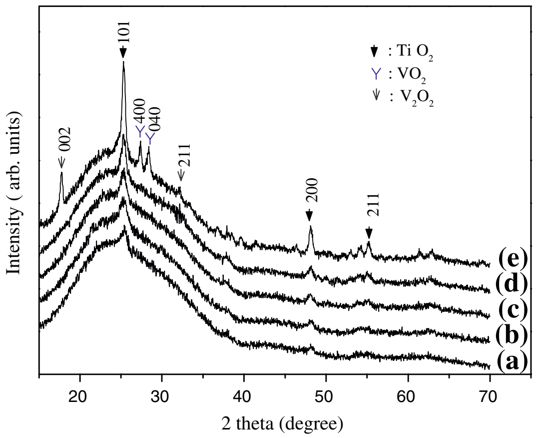

Fig. 1 XRD patterns of the V-doped TiO_2 thin films: (a) TiO_2, (b) VT001, (c) VT0025, (d) VT005, (e)VT01

two obvious diffraction peaks of VO_2 (orthorhomobic) 27.4°(400) and 28.3°(040) (PDF No.76-0676), the diffraction peaks of V_2O_5 (orthorhomobic) are also observed at 17.6°(002) and at 32.3°(211) (PDF No.85–2422). Based on the characteristics of (101) peak, the crystal size of anatase TiO_2 was obtained from the Scherrer's eq. [23]: $d_c = K\lambda / (\beta \cos\ \theta)$, where d_C is the size of the crystal, K is the Scherrer constant of 0.9, λ is the wavelength of X-ray radiation (0.15405 nm), β is the full width at half-maximum (FWHM) of selected peak, and θ is the diffraction angle for the selected peak. The crystal sizes for all the samples are listed in Table 1. It is obvious that the crystal size of anatase TiO_2 increases with the enhancement of V concentration in treatment solution.

In the aqueous solution of $(NH_4)_2$ TiF_6, TiF_6^{2-} ions hydrolyze into metal-fluoro complex ions as the following equilibrium scheme [24]:

$$[TiF_6]^{2-} + nH_2O \leftrightarrow [TiF_{6-n}(OH)_n]^{2-} + nHF \quad (1)$$

H_3BO_3 scavenges F from the$[TiF_{6\text{-}n}\ (OH)_n\ ]^{2-}$, and forms more stable complex ions, BF^{4-}, as follows [19]:

$$BO_3^{3-} + 4F^- + 6H^+ \rightarrow BF_4^- + 3H_2O \quad (2)$$

$[Ti(OH)_6]^{2-}$ ions form simultaneously. At the initial stage of the film growth, the nuclei of TiO_2 appear due to the dehydration reaction between OH^- groups existing on the surface of the substrate and $[Ti(OH)_6\ ]^{2-}$ ions near the substrate, which give rise to chemically-bonding between the films and substrate. Then, the dehydration reaction between the $[Ti(OH)_6\ ]^{2-}$ ions from the solution and OH^- groups on the newly-grown TiO_2-liquid interface forms the octahedral structures (TiO_6^{2-}). The agglomeration of a lot of TiO_6^{2-} octahedra causes the continuous growth of TiO_2 films. The as-deposited films are amorphous because of the rapid aggregation of TiO_6^{2-} octahedra. However, short-range orderly structures, similar to that in anatase TiO_2, may exist in as-deposited films [25]. After annealing, amorphous films were converted into anatase films. In the treatment solution, vanadium mostly exists in the form of fluoro-oxy complex ions ($[VOF_{n\text{-}x}\ (OH)_x]^{2\text{-}n}$) following the hydrolysis reaction [20]:

$$[VOF_n]^{2-n} + xH_2O \leftrightarrow [VOF_{n-x}(OH)_x]^{2-n} + xHF \quad (3)$$

Similarly, the equilibrium reaction (3) shifts to the right side because of the reaction (2) between F^- ions and a fluorine scavenger ($H_3\ BO_3$). Then, $[VO(OH)_n]^{2\text{-}n}$ species are generated. The dehydration reaction occurs between the $[VO(OH)_n]^{2\text{-}n}$ species, partially replacing the $[Ti(OH)_6]^{2-}$ species, and the hydroxyl groups on the newly-grown interface. Vanadium ions occupy some Ti sites of TiO_2, and the V-doped TiO_2 thin films grow continuously.

Since it is well known that the ionic radius of six-coordinated V^{4+} (0. 72 Å), than that of V^{5+} (0.68 Å), is closer to that of Ti^{4+} in TiO_2 (0.74 Å), it is concluded that V^{4+} ions are easier to substitute Ti^{4+} sites in TiO_2 lattice than V^{5+} [10, 12]. Many studies have proved the solid solubility between TiO_2 and VO_2 [11, 26]. A. Davidson et al. demonstrated the substitution of V^{4+} ions in TiO_2 rutile matrix by an ESR technique [26]. Furthermore, it has reported that the isolated mono-oxo vanadyl (not $V_2\ O_5$) centers exist on the surface of TiO_2 at low coverage [27, 28]. This indicates the strong dispersion ability of the surface of TiO_2 to V ions, which prevents to a certain extent the formation of pure vanadium oxides phases on the newly-grown interface of V-doped TiO_2 thin films in the LPD process. It may be reasonably deduced that V^{4+} is incorporated into the TiO_2 thin films by in-situ substituting Ti^{4+} site of TiO_2 in LPD process, not by forming vanadium oxides. With the increase of V amount in the V-doped TiO_2 films, as the sample VT01, the majority of V^{4+} ions remain in the TiO_2 matrix by substituting Ti^{4+} site of TiO_2, the excess of V^{4+} ions forms the pure VO_2 (as in Fig. 1). The appearance of $V_2\ O_5$ phase may be ascribed to the oxidation of VO_2 during the annealing.

The $V2p^{3/2}$ XPS spectra of V-doped films are shown in Fig. 2. The $V2p^{3/2}$ peak at ca. 516.6 eV appears for the sample VT001, which indicates the existence of V^{4+}

Table 1 Crystal size of anatase TiO_2 in V-doped TiO_2 thin films

Sample	FWHM (degree)	Crystal size (nm)
TiO_2	0.95	8.5
VT001	0.93	8.7
VT0025	0.786	10.3
VT005	0.621	13.1
VT01	0.4118	19.7

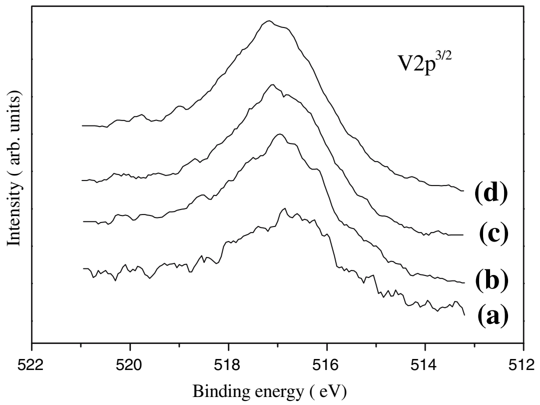

Fig. 2 V2p$^{3/2}$ XPS spectra of V-doped TiO_2 films: (**a**) VT001, (**b**) VT0025, (**c**) VT005, (**d**) VT01

[12, 28]. With increase of the V ions concentration in the treatment solution, a slight shift of V2p$^{3/2}$ peak was observed toward the higher binding energy side (from 516.6 eV of VT001 to 517.0 eV of VT01), indicative of the appearance of V^{5+} species in the film. The chemical states of vanadium in the V-doped TiO_2 thin films were analyzed in detail by the deconvolution using Gaussian mixture peak fitting. The deconvoluted XPS spectra for V2p$^{3/2}$ showed that the peak of V2p$^{3/2}$ in V-doped TiO_2 consists of two peaks at 516.6 eV, characteristic of V^{4+}, and at 517.3 eV, characteristic of V^{5+} [12, 28]. The relative contents of V^{4+}, V^{5+} in the total V ions are listed for all the samples in Table 2. The result shows that V in the V-doped TiO_2 films mostly exists in V^{4+} occupying the Ti^{4+} site of TiO_2 lattice. With the increase of V ions concentration in the treatment solution, the amount of V^{5+} in the V-doped TiO_2 films increases. By XPS spectra and ESR spectra of vanadium oxide on the titania, Miguel A. Banares et al. found that below theoretical surface monolayer coverage, V(χ) species is present on the surface of TiO_2 due to the strong interaction with TiO_2, which is ascribed to the remarkably close radii ratio [28]. In LPD process, V^{4+} ions in-situ substitute some Ti^{4+}ions of TiO_2 during the growth of films in the treatment solution with low V concentration, and the stable V-doped TiO_2 thin films were obtained (as the sample VT001). With the increase of V amount in the treatment solution, the amount of V^{4+} ions occupying Ti^{4+} sites of TiO_2 increases. Meanwhile, small VO_2 clusters appear due to the agglomeration of the excess VO species on the newly-grown interface. These small VO_2 clusters are then incorporated into the films. Due to the great thermal stability of Ti–O–V linkages [14, 29], V^{4+} ions occupying some Ti^{4+} sites remain in the TiO_2 lattice during the annealing. Whereas, the V^{4+} ions existing in the form of VO_2 clusters are partially oxidized into V^{5+} during the annealing, which causes the increase of V^{5+} ions in V-doped TiO_2 thin films (shown in Table 2). With further increase of V ions concentration in the treatment solution, highly-dispersed VO_2 clusters aggregate into larger clusters with short-range orderly structure. After annealing, the pure VO_2 crystals form. During annealing, some of VO_2 are oxidized into V_2O_5 because of containing-oxygen atmosphere, i.e. air. This is supported by the appearance of VO_2 and V_2O_5 phases in the sample VT01 (as in Fig. 1).

Table 2 The relative contents of V^{4+}, V^{5+} accounting for the total V ions in V/TiO_2 films

Sample	V^{4+}(at%)	V^{5+}(at%)
VT001	99.2	0.8
VT0025	95.8	4.2
VT005	76.3	23.7
VT01	62.4	37.6

The Ti2p XPS spectra of V-doped films are shown in Fig. 3. No apparent change of the peak position of Ti2p is observed for all the samples, and the Ti2p$^{3/2}$ peak is composed of a single one at 458.5 eV, corresponding to that of the Ti^{4+} oxidation state [30]. The shape and position of Ti2p exclude the obvious presence of the other oxidation states (Ti^{3+}) [31]. This indicates the chemical status of Ti in V-doped TiO_2 films is scarcely influenced by the introduction of V. G. Zhao et al., in their study of the sol–gel derived V-doped TiO_2 films, presented that cationic vacancies formed by Ti^{3+} moving to interstitial sites are the prerequisite to the introduction of V^{4+} ions into substitutional sites, and that Ti^{3+} ions are produced during heat-treatment due to the decomposition of organic compounds [11]. Different from the sol–gel process, in LPD process V^{4+} ions in-situ substitute Ti^{4+} ions on the newly-grown interface during the growth of film. The absence of the oxidation state of Ti^{3+} in XPS spectra (as in Fig. 3) supports the in-situ substitution mechanism for the LPD process.

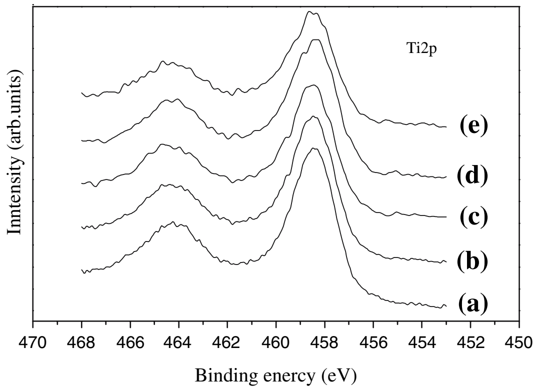

Fig. 3 Ti2p XPS spectra of V-doped TiO_2 films: (**a**) TiO_2, (**b**) VT001, (**c**) VT0025, (**d**) VT005, (**e**) VT01

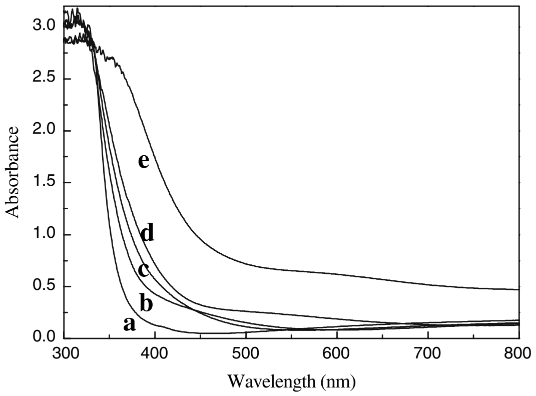

Fig. 4 UV-vis absorption spectra of the V-doped TiO_2 films: (**a**) TiO_2, (**b**) VT001, (**c**) VT0025, (**d**) VT005, (**e**) VT01

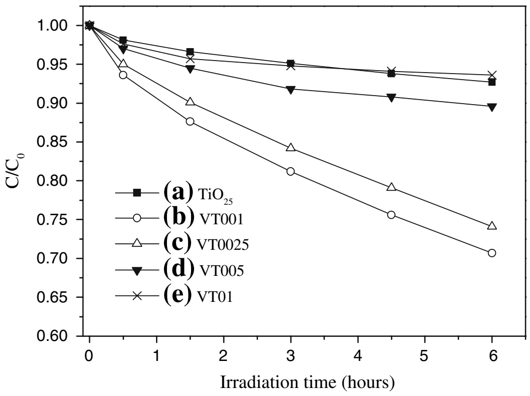

Fig. 5 Comparison of the photocatalytic decomposition of MB under visible light irradiation, catalyzed by (**a**) TiO_2, (**b**) VT001, (**c**) VT0025, (**d**) VT005, and (**e**) VT01

Figure 4 shows the photon absorbance of incident light vs. the wavelength for all the samples. It is clear that the UV-vis absorption spectra of V-doped TiO_2 thin films exhibit an obvious redshift comparing with the undoped TiO_2 films. The absorption edge shifted to a longer wavelength with the increase of V ions concentration. This indicates that the band gap of V-doped titanium dioxide films obviously decrease with the doping level. The band gap of a semiconductor could be modulated by incorporation of other semiconductors with different band gap, such as a mixed semiconductor $Ti_{1-x}Pb_xO_2$ [32]. Similarly, the introduction of other metal ions can change the electronic structure of TiO_2, and further affect its optical properties [7, 12]. The overlap of the 3d orbital of V^{4+} ions and the conduction band due to Ti3d of TiO_2 valence band narrows the band gap of dopedTiO_2, and devotes to the appearance of enhanced absorbance for the V-doped TiO_2 thin films in the visible region [7, 9, 27]. With the increase of V amount, the band gaps shift from 3.3 eV for the undoped TiO_2 films to 2.3 eV for the sample VT01. The existence of pure V_2O_5 phases, which was disclosed by the XPS measurements and the XRD pattern, partially accounts for great narrowing of the band gap of the sample VT01, and provides its obvious absorption even in the whole visible region.

The photocatalytic activity of V-doped TiO_2 films was evaluated by the de-colorization of MB solutions under visible light irradiation. The concentration of MB is obtained by the linear correlation between absorption and concentration of MB solution. Figure 5 shows the concentration change as the function of irradiation time. The decrease of the concentration of MB with the increase irradiation time indicates that the V-doped TiO_2 films are photoactlytically active under visible irradiation. The sample VT001 shows the best vis-photocatalytic activity. With further increase of V content from VT0025 to VT01, the vis-photocatalytic activity gradually weakens. For the sample VT01, the vis-photocatalytic activity is scarcely detected comparing to undoped TiO_2 thin films The detectable degradation rate for the pure TiO_2 is ascribed to a small fraction of residue UV irradiation from the ordinary incandescent lamp [33].

The photogenerated electron-hole pairs afford the possibility of photo-catalytic activity. By the aerobic mechanism presented by Ollis [6, 34], hydroxyl (OH) radicals are formed directly by photo-generated electron-hole pairs at the surface of catalysts under visible light irradiation. OH radicals decompose and mineralize MB, in contact with the surface of the V-doped TiO_2 films, into simple inorganic minerals (such as CO_2, NH_4^+, NO_3^-, SO_4^{2-}) [2, 35]. It should be noted that the enhanced absorption of a catalyst is a necessary condition for the vis-photoactivity, but not sufficient for that, as was observed in [36]. It is well known that active species, superoxide ($O_2^{\cdot-}$) radicals and hydroxyl ($OH^{\cdot}$) radicals are indispensable for the photo-decomposition reactions on the surface of TiO_2 [1, 2]. Their generation potentials, on the TiO_2 surface at pH 7, are respectively –0.28 eV for$O_2/O_2^{\cdot-}$ and +2.27 eV for $OH^{\cdot}/H_2O$ [2]. This indicates that the wavelength of irradiation should be less than a spectral limit (e.g. 486 nm assuming that one leaves out the energy necessary for photo-generated carriers to migrate towards the surface of TiO_2) of photocatalytic reaction in order to guarantee the formation of these photoactive species [37]. Though the outstanding absorption was observed for the sample VT01 even in the range of λ = 486–800nm (as in Fig. 4),the energy of photo-generated carriers duo to the irradiation in this region is not enough for the formation of these photoactive species ($O_2^{\cdot-}$, $OH^{\cdot}$). Furthermore, it has reported that V_2O_5 is detrimental to the photo-catalytic activity of V-doped TiO_2 thin films [12, 13]. The V_2O_5 phase in films may act as the recombination centers of photo-generated carriers. According to the XPS analysis, V ions in the sample VT001 exist in V^{4+}, not in V^{5+}, by in situ substituting Ti^{4+} site of TiO_2 lattice.

These V^{4+} ions enhance the vis-absorption of VT001, and provide VT001 with outstanding vis-photocatalytically activity. However, the redundant introduction of V ions gives rise to the increase of V^{5+} amount from the sample VT0025 to VT01. Increasing V^{5+} ions may cause the formation of highly-dispersed pure V_2O_5 phases, which act as the recombination centers of photo-generated carriers, and debase the vis-photocatalytically activity of VT0025, VT005, and VT01. For the sample VT01, detectable pure V_2O_5 phase recombines most of photo-generated carriers, and few of carriers, with energy enough to generate photoactive species ($O_2^{\cdot -}$, $OH^{\cdot}$), can migrate to the surface of films. Accordingly, no detectable vis-photocatalytic activity is observed.

4 Conclusions

The V-doped TiO_2 thin films have been successfully prepared through the LPD method. In this simple and easily-controlled process, V-doped anatase TiO_2 thin films were directly deposited on a soda lime glass substrate that is placed in an aqueous solution containing Ti- and V-fluoro complex ions, after annealing. V-doped TiO_2 thin films show outstanding vis-photocatalytic activity under the irradiation from an ordinary incandescent lamp. The enhanced vis-photocatalytic activity was attributed to the modification of the electronic structure of TiO_2 thin films through the in-situ substituting Ti^{4+} in the TiO_2 lattice with V^{4+} during the growth of films. Due to be low cost and very easily-controlled, this novel method is promising for the preparation of vis-photocatalytically active TiO_2 thin films doping with metal elements or nonmetal elements.

References

1. Carp O, Huisman CL, Reller A (2004) Prog Solid State Chem 32:33
2. Fujishima A, Rao TN, Tryk DA (2000) J Photochem Photobiol C: Photochem Rev 1:1
3. Fujishima A, Honda K (1972) Nature 238:37
4. Khan SUM, Al-Shahry M, Ingler WB Jr (2002) Science 297:2243
5. Asahi R, Morikawa T, Ohwaki T, Aoki K, Taga Y (2001) Science 293:269
6. Gole JL, Stout JD, Burda C, Lou Y, Chen X (2004) J Phys Chem B 108:1230
7. Umebayashi T, Yamaki T, Itoh H, Asai K (2002) J Phys Chem Solids 63:1909
8. Dvoranová D, Brezová V, Mazúr M, Malati MA (2002) Appl Catal B- Environ 37:91
9. Yamashita H, Harada M, Misaka J, Takeuchi M, Ikeue K, Anpo M (2002) J Photochem Photobiol A: Chem 148:257
10. Zhou JK, Takeuchi M, Zhao XS, Ray AK, Anpo M (2006) Catal Lett 106:67
11. Zhao GL, Kozuka H, Lin H, Yoko T (1999) Thin Solid Films 339:123
12. Iketani K, Sun RD, Toki M, Hirota K, Yamaguchi O (2004) Mat Sci Eng B-solid 108:187
13. Jimmy CY, Jun L, Raymund WM, Wok K (1997) J Photochem Photobiol A: Chem 111:199
14. Klosek S, Raftry D (2001) J Phys Chem B 105:2815
15. Forzatti P, Tronconi E, Busca G, Tittarelli P (1986) Catal Today 1:209
16. Briand LE, Bonette RD, Sanchez MA, Thomas HJ (1996) Catal Today 32:205
17. Kawahara H, Honda H (1984) Japanese patent 59141441 A (Nippon Sheet Glass), August 14
18. Sakai Y, Norimatsu H, Saito Y, Inomata H, Mizuno T (2001) Thin Solid Films 392:294
19. Masuda Y, Seo W-S, Koumoto K (2004) Solid State Ionics 172:283
20. Deki S, Aoi Y, Miyake Y, Gotoh A, Kajinami A (1996) Mater Res Bull 31:1399
21. Deki S, Kuratani K, Uemura M, Akamatsu K, Mizuhata M, Kajinami A (2004) Thin Solid Films 460:83
22. Jeffrey C-SW, Chen C-H (2004) J Photochem Photobiol A: Chem 163:509
23. Su C, Hong B-Y, Tseng C-M (2004) Catal Today 96:119
24. Shi Y-L, Zhang X-G, Li H-L (2002) Mat Sci Eng A-Struc 333:239
25. Gopal M, Chan WJM, Jonghe LCD (1997) J Mater Sci 32:6001
26. Davidson A, Che M (1992) J Phys Chem 96:9909
27. Larrubia MA, Busca G (2001) Mater Chem Phys 72:337
28. Ares MAB, Alemany LJ, Jime'nez MC, Larrubia MA, Delgado F, Granados ML, Martı'nez-Arias A, Blasco JM, Fierro JLG (1996) J Solid State Chem 124:69
29. Trifiro F (1998) Catal Today 41:21
30. Babelon P, Dequiedt AS, Moste'fa-Sba H, Bourgeois S, Sibillot P, Sacilotti M (1998) Thin Solid Films 322:63
31. Atashbar MZ, Sun HT, Gong B, Wlodarski W, Lamb R (1998) Thin Solid Films 326:238
32. Rahmana MM, Krishna KM, Soga T, Jimbo T, Umeno M (1999) J Phys Chem Solids 60:201
33. Kumar S, Fedorov AG, Gole JL (2005) Appl Catal B- Environ 57:93
34. Chen J, Ollis DF, Rulkens WH, Bruning H (1999) Wat Res 33:1173
35. Houas A, Lachheb H, Ksibi M, Elaloui E, Guillard C, Herrmann J-M (2001) Appl Catal B- Environ 31:145
36. Davydov L, Reddy EP, France P, Smirniotis PG (2001) J Catal 203:157
37. Lia D, Haneda H, Hishita S, Ohashi N, Labhsetwar NK (2005) J Fluorine Chem 126:69